J|A|C|S
COMMUNICATIONS

Published on Web 08/16/2003

Vapor Phase Synthesis of Tungsten Nanowires

Sreeram Vaddiraju, Hari Chandrasekaran, and Mahendra K. Sunkara*

Department of Chemical Engineering, University of Louisville, Louisville, Kentucky 40292

Received April 30, 2003; E-mail: mahendra@louisville.edu

Vapor phase methods for synthesizing metal nanowires directly without the help of templates have not been studied extensively. Even though there have been few reports with one dating back to 1877 on metal whisker synthesis from the vapor phase, the inconclusive growth mechanism did not lead to any serious developments for nanowires.[1] Recently, there are also two reports with one using hydrogen on tungsten oxide for tungsten nanowires, and another using decomposition of tungsten complexed organic precursors for amorphous carbon sheathed, polycrystalline tungsten nanowires.[2]

In this context, we report a novel method in which nucleation and growth of metal oxides at temperatures higher than the oxide decomposition temperatures lead to the respective metal nanowires. Specifically, we demonstrate this concept with the bulk synthesis of tungsten nanowires. The chemical vapor transport of tungsten in the presence of oxygen onto substrates kept at temperatures higher than the tungsten oxide decomposition temperature (∼1450 °C) led to nucleation and growth of pure metallic tungsten nanowires. The vapor transport of low-melting metal oxides is a known procedure for metal-oxide ribbons, whiskers,[3] and recently for nanobelts and nanowires.[4] It is not known for synthesizing metal nanowires. Nanowires of transition metals could find applications in electronic devices, sensors, and magnetic recording devices and also show interesting structural and electronic characteristics.[5]

The chemical vapor transport experiments were performed using a modified HF-CVD reactor in which substrates were placed close to the filaments (0.5 mm diam) at a distance of 1 mm or less. O_2 flow rate was varied from 0.03 to 0.1 sccm in 90 sccm of either N_2 or Ar. Experiments were performed at different filament temperatures ranging from 1200 to 2000 °C and at a pressure of 150 mTorr.

The scanning electron micrographs of the tungsten nanowires resulting from the chemical vapor transport of tungsten from tungsten filaments at a temperature of 1750 °C with 0.03 sccm of O_2 in 90 sccm of N_2 are shown in Figure 1. The tungsten filament made contact with the substrate at the edges of region 1. The regions (a few millimeters on either side of the filament) closest to filament showed high densities of nanowires. In region 1 which is very close (< ∼1 mm) to the filament, crystals of tungsten are observed as depicted in Figure 1a. Tapered (Figure 1b) and straight (Figure 1c) nanowires of tungsten are observed in regions 2 and 3, respectively. In some instances, the tungsten nanowires joined together and appeared as sheetlike structures, as seen at a few places in Figure 1c. Region 4, which is farther away from the filament on the substrate, exhibited nanocrystalline tungsten oxide deposit. The diameter of the resulting nanowires ranged from 55 nm at a filament temperature of 1750 °C to as low as 40 nm at 2000 °C and are a few micrometers long. The resulting density of the nanowires was approximately 10^8-10^9 cm^{-2}. The results did not show any dependence on the substrate used, that is, pBN or quartz, indicating no role of substrate material on the growth of nanowires.

A low magnification TEM image (Figure 1d) indicates no tapering of the nanowires found in region 3. The majority of the nanowires were straight without any apparent tapering at the end

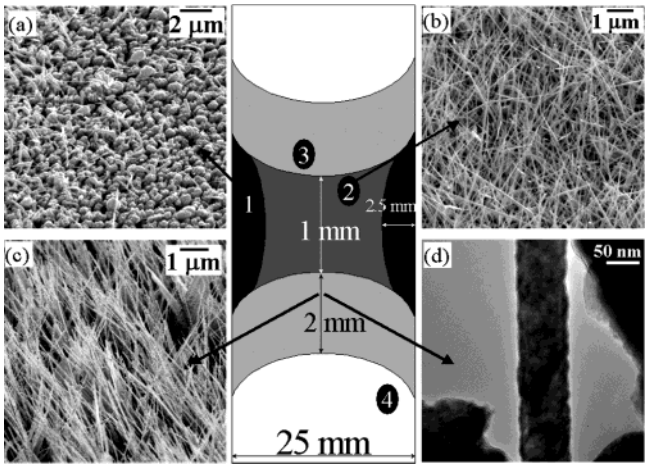

Figure 1. SEM images showing (a) formation of tungsten crystals in region 1, (b) formation of tapered nanowires in region 2, (c) formation of straight nanowires in region 3, and (d) low magnification TEM micrograph of a straight nanowire from region 3. The regions on the substrate where they are formed are also indicated.

and without any cluster at the tip. A high-resolution TEM (Figure 2a) indicates that the nanowires are single crystalline with no amorphous or oxide sheath at the edges and that the growth direction is [110] (Figure 2b). The XRD pattern (Figure 2c) of the as-synthesized sample at 1750 °C shows diffraction peaks corresponding to two phases, metallic tungsten from regions 1, 2, and 3 and monoclinic tungsten trioxide from region 4.

The chemical vapor transport experiments onto substrates at a temperature of 1250 °C produced only polycrystalline tungsten trioxide according to XRD and SEM analysis (no data included). This indicates that the growth of tungsten nanowires does not occur by the decomposition of the already formed tungsten trioxide nanowires, but decomposition of tungsten trioxide to tungsten is a necessary step for 1-D growth during the process. Experiments conducted by placing a second substrate at a distance around 5−8 mm from the filament formed both tungsten trioxide nanowires and nanotubes. No tungsten nanowires were formed on this substrate. The temperature of this substrate, heated primarily by radiation, is ∼800 °C. Initial analysis of this sample using XRD and TEM showed the presence of monoclinic WO_3 nanowires and nanotubes. The results with tungsten oxide nanowires are consistent with other recent reports on treelike structures[6] and nanowires,[7] but nanotube results are completely surprising. In-depth characterization is currently being performed and will be reported later.

We hypothesize that the nucleation and growth of tungsten nanowires occurs by the following mechanism. The WO_2 vapor phase species is formed in the presence of oxygen. Nucleation of WO_2 on the substrate occurs due to supersaturation of WO_2(v) in the gas phase. For condensation of the vapor phase species, the critical nuclei diameter, d_c, depends on the supersaturation by the relation[8]

$$d_c = 4\sigma\Omega/[RT \ln(p/p^*)] \quad (1)$$

10.1021/ja035868e CCC: $25.00

where σ is the interfacial energy, Ω is the molar volume, T is the temperature of the substrate, p is the partial pressure of the growth species, and p^* is the vapor pressure of the growth species at equilibrium. Both p and p^* are functions of temperature. As the filament temperature increases, the supply of the participating vapor phase species, that is, p, increases along with the increase in p^*.

To determine the effect of temperature, we performed several experiments at different filament temperatures ranging from 1500 to 2000 °C. The temperature of the substrate that is less than 1 mm distance from the filament is considered to be equal to that of the filament. Preliminary evidence suggests that, as the temperature is increased from 1500 to 2000 °C, the diameter of the nanowires reduced from 70 to 40 nm, while increasing the nucleation density. As the temperature is increased, the ratio p/p^* seems to remain constant. So the critical nuclei diameter is inversely proportional to temperature, leading to the formation of wires of smaller diameter at higher temperatures. An increase in the amount of oxygen from 0.03 to 0.1 sccm increased the growth rates from 1 to 10 μm/h. The analysis using the thermodynamic data from NASA database[9] suggests that the formation of WO_2(v) species is quite spontaneous.

$$W + O_2 \rightarrow WO_2(v) \quad \Delta G = -40.08 \text{ kJ/mol K (1450 °C)} \quad (2)$$

Similarly, tungsten trioxide vapor phase species could also be formed simultaneously. Yet, the gas−solid equilibrium calculations in the presence of tungsten oxide solid phases indicate that tungsten dioxide is the primary vapor phase species. The condensation of the tungsten dioxide species takes place both in the nucleation stages and in the further growth process as adatoms. The adatoms undergo subsequent decomposition to tungsten at high temperatures (closer to the filament).

$$WO_2(v) \rightarrow W(s) + O_2 \qquad \Delta G = -267.33 \text{ kJ/mol K (1500 °C)} \quad (3)$$

$$WO_3(v) \rightarrow W(s) + {}^3/_2O_2 \qquad \Delta G = -360.32 \text{ kJ/mol K (1500 °C)} \quad (4)$$

Farther away from the filament, tungsten dioxide adatoms transform into tungsten trioxide species. Because of the lower temperature, further decomposition is absent, thus giving tungsten trioxide 3-D nanocrystallites.

$$WO_2(s) + {}^1/_2O_2 \rightarrow WO_3(s) \qquad \Delta G = -108.24 \text{ kJ/mol K (1000 °C)} \quad (5)$$

The growth in 1-D is accomplished by the preferential condensation of tungsten oxide on preexisting tungsten oxide at the tip of the nanowire and the subsequent decomposition of tungsten oxide to tungsten. At high temperatures (very close to the filament), the net rate of decomposition is higher than the rate of condensation, giving rise to the tapering observed in nanowires found in region 2 (Figure 1b). Similarly, at slightly lower temperatures (slightly away from the filament), but higher than the decomposition temperature, the net rate of decomposition is similar to the rate of condensation, allowing uniform diameter (Figure 1c). At regions far away from the heat source, where the temperature is below the decomposition temperature, WO_3 does not decompose as observed in the XRD pattern and deposits as nanocrystalline tungsten oxide powder. The synthesis temperature may be lowered in the presence of a reducing agent like H_2.

In conclusion, we have successfully demonstrated a vapor phase technique in which condensation of oxide species above their decomposition temperatures leads to the growth of metal nanowires. Increasing temperatures beyond the decomposition temperature reduced the diameter of the nanowires. This technique may be extended to the synthesis of other metal nanowires such as Fe, Ta, Ti, Cu, etc.

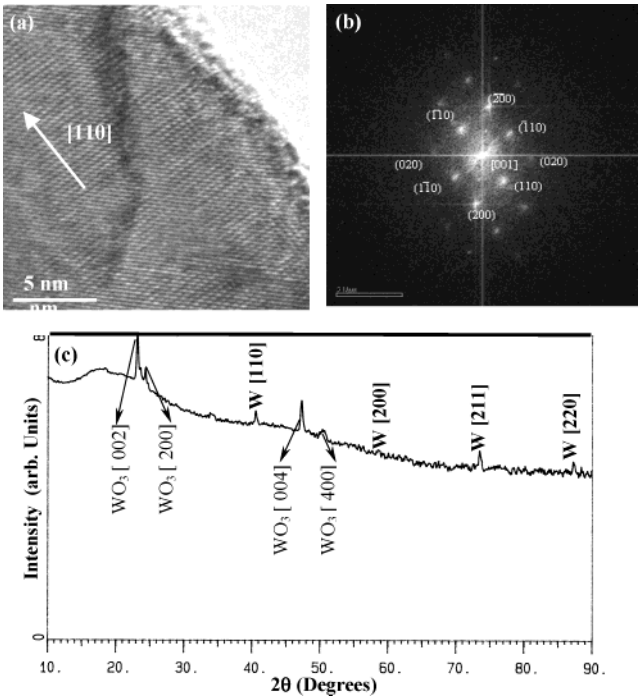

Figure 2. Diffraction patterns from the obtained nanowires. (a) and (b) TEM diffraction pattern showing BCC crystal structure corresponding to tungsten. The growth direction is [110]. (c) XRD diffraction pattern showing primary reflections corresponding to that of tungsten (WO_3 reflections are from parts of the substrate at low temperature).

Acknowledgment. The authors thank Prof. E. Gulari (U. Michigan) for donating a complete HF CVD reactor, and Dr. S. Harfenist (U. Louisville) and Dr. W. Xu (UK) for help with SEM and JEOL 2010f. The authors acknowledge partial support from NSF (CTS 9876231) and AFOSR (F49620-00-1-0310).

Supporting Information Available: EDS, XRD spectra, SEM images of the tungsten nanowires, and 3-D crystallites observed in region 1 (PDF). This material is available free of charge via the Internet at http://pubs.acs.org.

References

(1) (a) Margottet, J. *Compt. Rend*. **1877**, *85*, 1142. (b) Kittaka, S.; Kishi, K.; Kaneko, T. *J. Cryst. Growth* **1971**, *11*, 197. (c) Kitano, Y.; Komura, Y.; Iwanari, T.; Kurashige, R. *J. Cryst. Growth* **1974**, *24/25*, 354. (d) Nittino, O.; Hasegawa, H.; Nagakura, S. *J. Cryst. Growth* **1977**, *42*, 175. (e) Kaneko, T. *J. Cryst. Growth* **1978**, *44*, 14.
(2) (a) Li, Y.-H.; Choi, C.-H.; Jang, Y.-T.; Kim, E.-K.; Ju, B.-K. *Appl. Phys. Lett*. **2002**, *81*, 745. (b) Thong, J. T. L.; Oon, C. H.; et al. *Appl. Phys. Lett.* **2002**, *81*, 4823.
(3) Sharma, S.; Li, H.; Chandrasekaran, H.; Mani, R. C.; Sunkara, M. K. In *Encylcopedia of Nanoscience and Nanotechnology*; Nalwa, H., Ed.; American Scientific Publishers: Los Angeles, CA, 2003; and references within.
(4) Pan, Z. W.; Dai, Z. R.; Wang, Z. L. *Science* **2001**, *291*, 1947.
(5) (a) Walter, E. C.; Ng, K.; Zach, M. P.; Penner, R. M.; Favier, F. *Microelectron. Eng.* **2002**, *61−62*, 555. (b) Chou, S. Y.; Wei, M. S.; Krauss, P. R.; Fischer, P. B. *J. Appl. Phys.* **1994**, *76*, 6673. (c) Tosatti, E.; Prestipino, S. *Science* **2000**, *289*, 561−563. (d) Lin, Y.-M.; Cronin, S. B.; Ying, J. Y.; Dresselhaus, M. S.; Heremans, J. P. *Appl. Phys. Lett.* **2000**, *76*, 3944.
(6) Zhu, Y. Q.; Hu, W.; et al. *Chem. Phys. Lett*. **1999**, *309*, 327.
(7) Liu, Z.; Bando, Y.; Tang, C. *Chem. Phys. Lett*. **2003**, *372*, 179.
(8) Tiller, W. A. *The Science of Crystallization: Microscopic Interfacial Phenomena*; Cambridge University Press: New York, 1991.
(9) NASA Glenn Thermodynamic Database, http://cea.grc.nasa.gov.

JA035868E